International Journal of Recent Technology and Engineering (IJRTE)
ISSN: 2277-3878 (Online), Volume-8 Issue-2, July 2019

PV and Grid interfaced Plug-in EV Battery Charger operating in P-VG, P-V and V-G Modes

Partha Sarathi Subudhi, Krithiga S.

Abstract*: *The proposed system facilitates uninterruptable charging of a photovoltaic (PV) fed plug-in electric vehicle (EV) battery charging system irrespective of solar irradiation conditions by integrating utility grid to the battery charging system. The system employs bidirectional cycloconverter (BDCC) in order to use utility grid as source or sink during different modes of operation which depends on the availability of solar power. During low irradiation condition, the utility grid acts as a backup source in order to facilitate uninterruptable charging of the EV battery. When surplus power is generated from the PV panel, it is fed to the utility grid, which acts as sink in this mode. For uninterruptable EV battery charging, the controller operates the switches and relays in the proposed system corresponding to solar irradiation level. The available literatures define complex control strategies which are solved in this proposed system by adopting a simple dynamic control algorithm. The simulation of the proposed system has been carried out using PSIM simulation software and experimental prototype has been designed, developed and tested for different modes of operations to validate the efficacy of the proposed system.

Index Terms*: *Battery charging system, Bidirectional cycloconverter, Grid integration, Photovoltaic power generation, Plug-in electric vehicle .

I. INTRODUCTION

Increasing demand of electric vehicle (EV) over internal combustion engine vehicles led researchers to develop an efficient EV battery charging system [1]. Electric vehicles produce no poisonous by product which enables it to act as an alternative to the conventional transportation systems. Integration of non-conventional renewable energy sources with EV battery charging system provides a breakthrough in EV research sector [2]. Among all the renewable sources available, photovoltaic (PV) module is efficient due to its cost effectiveness, availability and no poisonous by product during operation [3]. Therefore, integration of PV with EV battery charging systems adds more advantages to the EV battery charging research area [4].

Most of the problems faced by petroleum and coal products can also be reduced if energy generated through PV cells is utilized to charge EV battery [5]. However, PV module has a limitation of producing power during night time but PV module power can be utilized efficiently by integrating it with a grid to supply the EV battery during non-peak sunshine hours [7]. In order to integrate the PV module with the EV battery charging system, power electronic converters are employed. These interfaces are also known as battery chargers [8-9].

With respect to the converter placement inside the EV or at the charging station, EV battery chargers are classified as ON board chargers and OFF board chargers [10-11]. The power electronic converters are placed inside the EV in case of ON board chargers, whereas, the converters are placed in the charging station in case of OFF board chargers. Different parameters such as vehicle weight, charger maintenance and safety measures made OFF board chargers more efficient than the ON board chargers. Therefore, the proposed work aims to design and develop a grid integrated PV powered OFF board plug-in EV battery charging system. Contributions of the proposed plug-in EV battery charging system are summarized as follows:

- An improved plug-in EV battery charger is proposed which supply uninterrupted power irrespective of solar irradiation level either from PV array or from utility grid.
- An improved automatic controller is proposed in this research article which controls the power flow in PV array to EV and grid (P-VG mode), PV array to EV (P-V mode) and grid to vehicle (G-V mode) with respect to solar irradiation level.

This paper consists of four sections. Section 1 & 4 deal with the introduction to the proposed system and conclusion of the paper respectively. Working of the proposed system in described in section 2. Simulation and experimental investigation of the plug-in EV battery charger is explained in section 3.

II. PROPOSED EV BATTERY CHARGER

The proposed charger enables uninterruptable charging of an EV battery. Fig.1 shows the schematic diagram of the proposed EV battery charger. The charger consists of PV panel, high frequency inverter (HFI), diode bridge rectifier, boost converter, high frequency transformer (HFT), bidirectional cycloconverter (BDCC) and utility grid. Operation of the proposed EV battery charger is provided in the following subsection.

Revised Manuscript Received on 30 July 2019.
***** Correspondence Author
Partha Sarathi Subudhi*, School of Electrical Engineering, Vellore Institute of Technology (VIT), Chennai, India.
Krithiga S., Corresponding author, School of Electrical Engineering, Vellore Institute of Technology (VIT), Chennai, India.

A. Description of the proposed EV battery charger

In this system, DC power is generated from the solar irradiation by employing PV module.

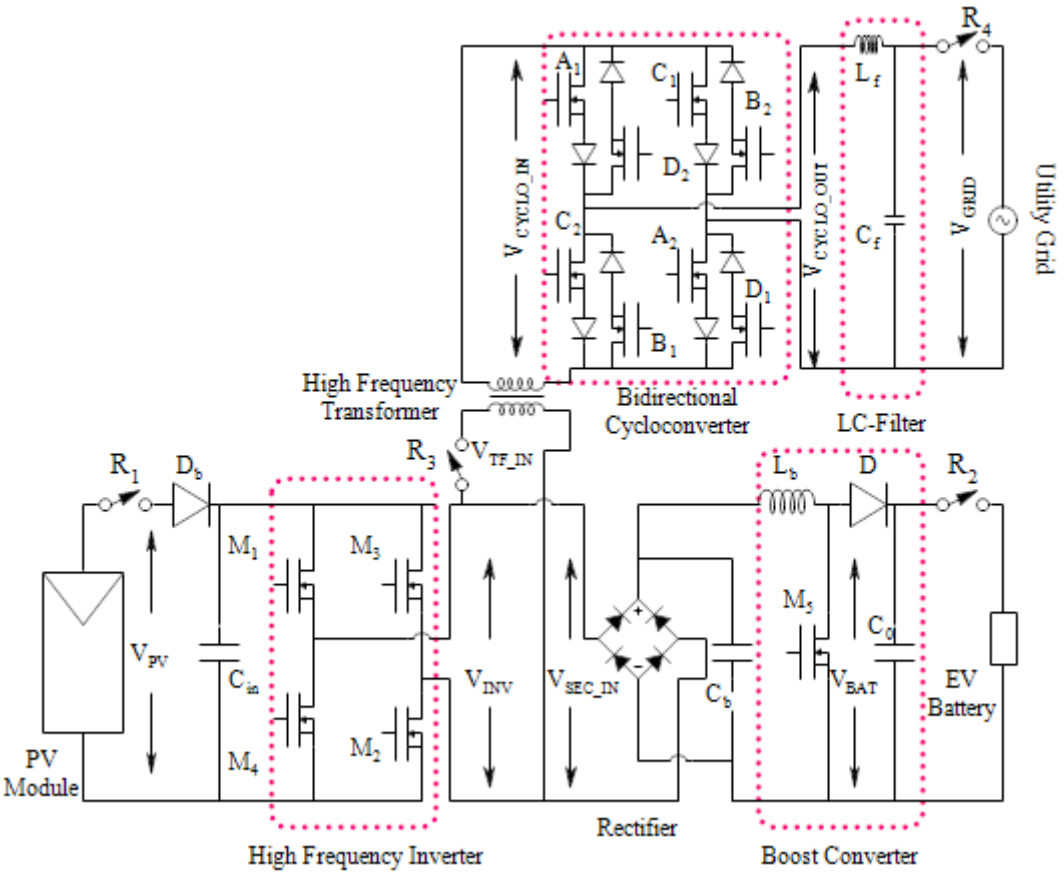

Figure 1. Schematic diagram of the proposed EV battery charger

A HFI circuit converts this generated dc voltage to high frequency ac voltage (HFAC). Utilizing HFI has an advantage of reducing the size of passive components in the circuits. The high frequency ac voltage is converted to dc voltage using the diode bridge rectifier and fed to the boost converter. Boost converter boosts the dc voltage to the required voltage, sufficient for charging the EV battery. In the proposed charger, a HFT and BDCC is used for transferring the power to utility grid from PV panel during higher irradiation conditions. For matching the grid voltage and frequency, with the HFI output voltage and frequency, a HFT and a BDCC is employed respectively. The transformer acts as a step up transformer in P-VG mode and step down for G-V mode. The HFT also provides isolation between the HFI and BDCC. The proposed charger is operated in three modes for supplying uninterruptable power to EV battery. During mode 1, i.e. at high irradiation condition, as surplus power is generated from the PV panel, excess power is fed to the utility grid in addition to charging of EV battery. This mode is referred as P-VG mode. In this mode, all the relays R_1, R_2, R_3 & R_4 remain closed. During mode 2 (P-V mode), when the PV panel generated power is sufficient only to charge the EV battery, utility grid and BDCC is isolated from the system by opening the relays, R_3 & R_4. During mode 3 (G-V mode), when the PV panel generated power is not enough to charge the EV battery, the PV panel is isolated from the proposed system by opening relay R_1 and EV battery is charged from the utility grid by operating the BDCC in reverse mode and closing the relays R_2, R_3 & R_4. During any of these modes, when the EV battery is fully charged, relay, R_2, is opened in order to avoid the overcharging of the EV battery.

B. Modes of operation of the EV battery charger

This section explains the different modes of operations of the EV battery charger at different solar irradiation conditions.

1. Mode 1: Forward PV- vehicle & grid connected mode of the proposed EV battery charger (P-VG)

In this mode, the PV module generates surplus power in order to charge the EV battery as well as to feed the excess power to the utility grid. The HFI output power is stepped up to match the grid voltage using HFT. Then, high frequency stepped up ac voltage, V_{CYCLO_IN} is converted to grid frequency using BDCC. In this mode, BDCC works in forward direction. For the positive half cycle of V_{CYCLO_IN}, the switches, A_1 and A_2 of BDCC as shown in Fig. 1 are in ON condition and other switches remain in OFF state. The current flows through the path, HFT secondary terminals - A_1- LC filter- grid- A_2- HFT secondary terminals. The voltage, V_{CYCLO_IN} is reflected across the BDCC output terminals. In the negative half cycle (-HC) of the voltage, V_{CYCLO_IN}, switches, B_1 and B_2 are in ON conditions whereas other switches remain in OFF state. The input current flows through the path, HFT secondary terminals - B_1 - LC filter- grid - B_2- HFT secondary terminals.

Retrieval Number: B2680078219/19©BEIESP
DOI: 10.35940/ijrte.B2680.078219
Journal Website: www.ijrte.org

Published By:
Blue Eyes Intelligence Engineering
& Sciences Publication

During this mode, the voltage, V_{CYCLO_IN} is reflected across the output terminals of the BDCC in opposite polarity, i.e. rectified output voltage. The above two condition results in positive half cycle (+HC) of cycloconverter output voltage. In order to generate the -HC of cycloconverter output, the switches, C_1 and C_2 are in ON conditions whereas other switches remain in OFF state during +HC of V_{CYCLO_IN}. The current flows through the path, HFT secondary terminals - C_1- LC filter- grid - C_2- HFT secondary terminals. The voltage, V_{CYCLO_IN} is reflected across the BDCC output terminals in opposite polarity. In the -HC of the voltage, V_{CYCLO_IN}, switches, D_1 and D_2 are in ON conditions whereas other switches remain in OFF state. The current flows through the path, HFT secondary terminals - D_1- LC filter- grid - D_2- HFT secondary terminals. During this mode, the voltage, V_{CYCLO_IN} is reflected across the output terminals of the BDCC. The above two condition results in -HC of BDCC output. In this way, the HFAC voltage is converted to LFAC voltage and fed to the utility grid.

In order to charge the EV battery, during P-VG mode, the high frequency voltage from the output terminals of the HFI is fed to a diode bridge rectifier which converts the high frequency voltage to dc voltage. The rectifier output voltage is stepped up using a boost converter sufficient enough to charge the EV battery.

2. Mode 2: PV-EV standalone mode operation of the proposed system (P-V mode)

This mode refers to normal irradiation condition in which PV panel generated power is sufficient only to charge the EV battery. The utility grid and the BDCC are isolated from the proposed system by opening relays R_3 and R_4. Hence, the EV battery is charged from the power generated from the PV panel only. PV panel generated power is converted to high frequency ac voltage using an HFI. During this mode, switches M_1 & M_2 of the HFI shown in Fig. 1 conducts in order to generate the +HC of the output ac voltage while M_3 & M_4 remain in off state. In order to generate the -HC of the output ac voltage, switches M_3 & M_4 conducts and M_1 & M_2 remain in off state. This HFAC is converted to dc using the diode bridge rectifier which is boosted using a boost converter in order to charge the EV battery.

3. Mode 3: Grid- EV reverse mode operation of the proposed EV battery charging system (G-V mode)

This mode comes into effect during non-sunshine hours either when the irradiation is lower or during night. In this mode, utility grid power is used to supply power to the EV battery as the relay, R_1 is opened to isolate the PV panel from the proposed system. During this interval, the grid voltage, V_{grid} passing through L & C acts as input voltage, V_{CYCLO_OUT} to the BDCC in reverse mode. The grid frequency voltage is converted to HFAC voltage in this mode by operating the BDCC in reverse mode [12-13]. In BDCC as shown in Fig.1, when the switches D_1 and D_2 are in ON state, the grid current flows through the path, grid- D_2- HFT secondary terminals - D_1- grid. During this interval, V_{CYCLO_OUT} is reflected across the secondary side of HFT terminals as +HC of the voltage, V_{CYCLO_IN}. In order to generate the +HC of the HFAC at the HFT secondary terminals, the switches C_1 & C_2 are kept in ON state. The utility grid current flows in a direction, grid- L- C_2- secondary side of HFT terminals - C_1 - grid in order to generate the negative half cycle voltage of the high frequency voltage at secondary terminals of the HFT. In the same manner, the switches B_1 & B_2 conducts to generate the +HC of the high frequency voltage at the secondary terminals of the HFT and A_1 & A_2 are kept ON state to generate the -HC of the high frequency ac voltage at the HFT secondary terminals.

An automatic controller is implemented in this system to control the power flow direction and generate pulses to operate the system in all the three modes. The following subsection explains the controller of proposed system.

C. Working of the controller

Four different controllers are designed for the operation of the system viz. relay controller, inverter controller, BDCC controller and boost converter controller. Working of each controller is explained in this section.

1. Relay Controller

PV panel output voltage and current changes throughout the day as a result of variation in solar irradiation level [14-15]. However, EV battery has to be charged constantly irrespective of the PV panel irradiation condition. Whenever, the actual irradiation, I_{rr} is greater than the irradiation upper limit, I_{rrH}, PV panel produces surplus power which helps in simultaneous feeding of power to EV battery and grid. The irradiation level below which the PV panel generated power is not sufficient to charge the EV battery is denoted by I_{rrL}. The controller decides the mode of operation of the system as per the solar irradiation level by operating the relays used in the proposed system. Block diagram of the relay controller is provided in Fig. 2. When the actual irradiation, I_{rr} is greater than I_{rrH}, the forward P-VG mode is activated by setting the $V_{fwdgrid}$ signal high. During mode 2, PV – EV standalone mode is activated when the actual irradiation value, I_{rr} lies between I_{rrH} and I_{rrL} by setting the V_{pvev} signal high. During mode 3, G-V mode is activated by setting the $V_{revgrid}$ signal high. All these modes are into effective stage only when the battery voltage, V_{bat} is less than the rated full charged voltage, V_{fc} i.e when the signal, S is high. During battery full charged mode, all the relays are kept in open state. The relays R_1, R_2, R_3 and R_4 are operated with the help of the generated control signals V_{gR1}, V_{gR2}, V_{gR3} and V_{gR4} as shown in Fig. 2. Operations of relays during the different modes are shown in Table 1.

2. Inverter controller

Gate pulses, V_{sw} with 50 % duty ratio are generated at a HF of 55 kHz and provided to the MOSFET switches of the HFI. This frequency is chosen to reduce the size of the HFT used in the proposed system. Switches M_1 and M_2 are provided with the same gate pulse, V_{sw} while M_3 and M_4 are provided with the 180º phase shifted pulses.

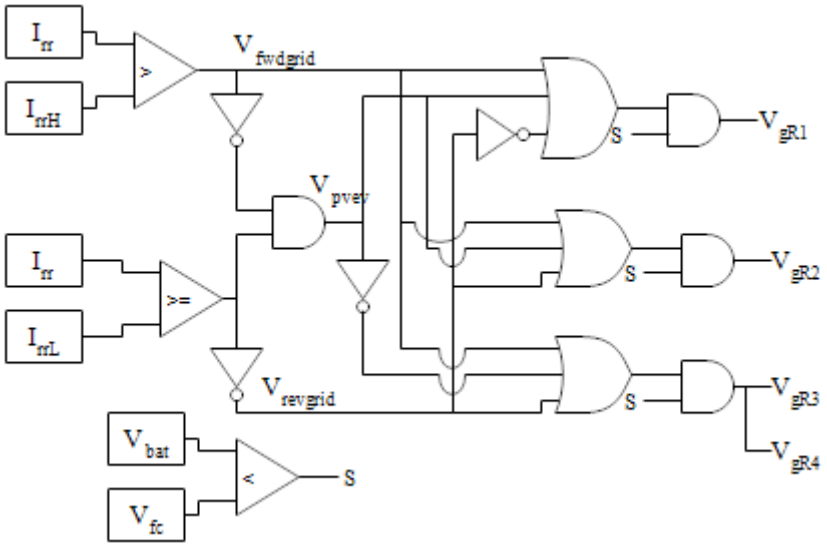

Figure 2. Block diagram of the proposed relay controller

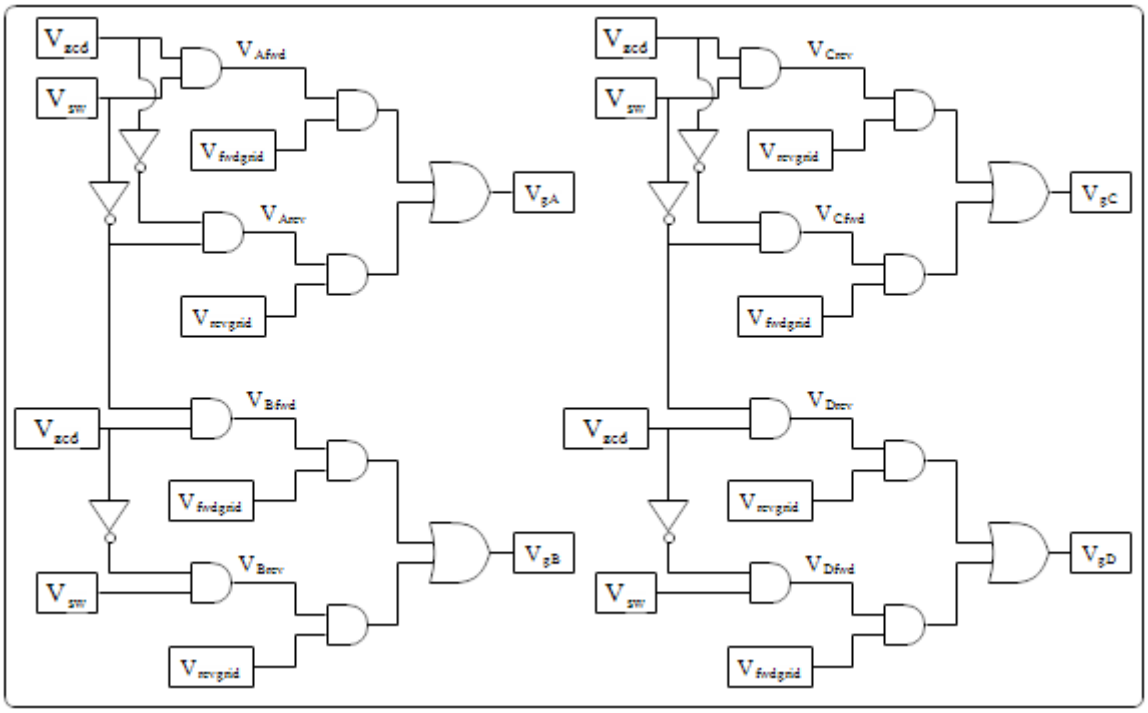

Figure 3. Operation of the proposed BDCC controller

Table 1. Operation of relays during different modes

Modes	R_1	R_2	R_3	R_4
Forward PV- vehicle & grid connected mode (P-VG)	ON	ON	ON	ON
PV-EV standalone mode (P-V)	ON	ON	OFF	OFF
Grid- EV reverse mode (G-V)	OFF	ON	ON	ON
Battery fully charged mode	OFF	OFF	OFF	OFF

1. BDCC controller

In order to integrate utility grid with the proposed system, synchronization with grid must be taken care of. The proposed controller operates the switches of the BDCC in order to facilitate smooth grid integration of the system. Working of the controller for forward and reverse modes of BDCC is shown in Fig. 3. V_{zcd} indicates the zero crossing detectors (ZCD) signal generated from the utility grid voltage using step down transformer and Opamp. The high frequency gate pulse, V_{sw} given to the HFI is inserted into the V_{zcd} signal for generating signal V_{AFwd}. When the mode 1 is activated, $V_{fwdgrid}$ signal is high state. This helps in passing the V_{AFwd} signal to operate switches A_1 and A_2 by generating gate pulse, V_{gA} as shown in Fig. 3. During mode 3, i.e G-V mode, $V_{revgrid}$ is in high state which helps in passing the signal, V_{ARev} to operate switches A_1 and A_2 as shown in Fig. 3.

V_{ARev} is generated by inserting the inverted V_{sw} signal into inverted V_{zcd} signal for operating A_1 and A_2 switches in -HC of the HFAC at the HFT secondary terminals. Similarly, the gate pulses, V_{gB}, V_{gC} & V_{gD} are generated for operating switches B, C & D respectively of BDCC as shown in Fig. 3.

2. Boost converter controller

In order to charge the EV battery, constant voltage is applied at the output terminals of the boost converter. A PI controller is used in this proposed system for maintaining the constant output voltage. An error signal is generated by comparing the boost converter output voltage with the reference voltage and fed to the PI controller. The reference voltage is the voltage greater than the nominal voltage of the EV battery. The PI controller generate reference signal which is again compared with the high frequency carrier signal in order to generate the gate pulse for the boost converter MOSFET.

III. SIMULATION STUDIES AND EXPERIMENTAL INVESTIGATION OF THE PROPOSED EV BATTERY CHARGER

Simulation analysis of the proposed EV battery charger is carried out using PSIM software and the experimental investigation of the proposed charger was performed by fabricating a laboratory prototype. The simulation studies of the proposed system with the experimental investigation results are provided in this section. PV module present in PSIM library is used as the source for the proposed system. The 250 W PV module is operated at 850 W/m^2 irradiation which delivers 200 W power.

Simulation study of the proposed EV battery charging system behavior during forward PV-EV and grid (P-VG) connected mode operation is carried out and the simulation waveforms are presented in Fig. 4, 5 and 6.

Fig. 4(a) indicates the PV module voltage and current of the proposed system during forward PV-EV & grid connected mode which are found to be 28.87 V and 6.9 A respectively. The HFI output voltage and current waveforms during P-VG mode are presented in Fig. 4(b) which are observed as 28.6 V and 6.98 A respectively. The HFI output power is fed to the rectifier and the HFT. The rectifier input voltage and current waveforms are presented in Fig. 5(a) which are observed as 28.6 V and 3.85 A respectively. The filtered rectifier output voltage and current waveforms are presented in Fig. 5(b) which are observed as 26.74 V and 3.92 A respectively. EV battery voltage and current waveforms are presented in Fig. 5(c) which are observed as 50.48 V and 2.03 A respectively. From the simulation study results, it is observed that, rectifier output voltage of 26.74 V is boosted to 50.48 V employing the boost converter in order to charge the EV battery. HFT primary side voltage and current waveforms are shown in Fig. 6(a) which are found to be 28.6 V and 3.13 A respectively. Secondary side of the HFT is connected to the input terminals of the cycloconverter.

Voltage and current waveforms of the BDCC input terminals are shown in Fig. 6(b) which are found to be 232.5 V and 0.385 A respectively. From Fig. 6(a) and 6(b), it is found that using HFT, the transformer primary side voltage of 28.6 V is stepped up to 232.5 V at the secondary side of the transformer.

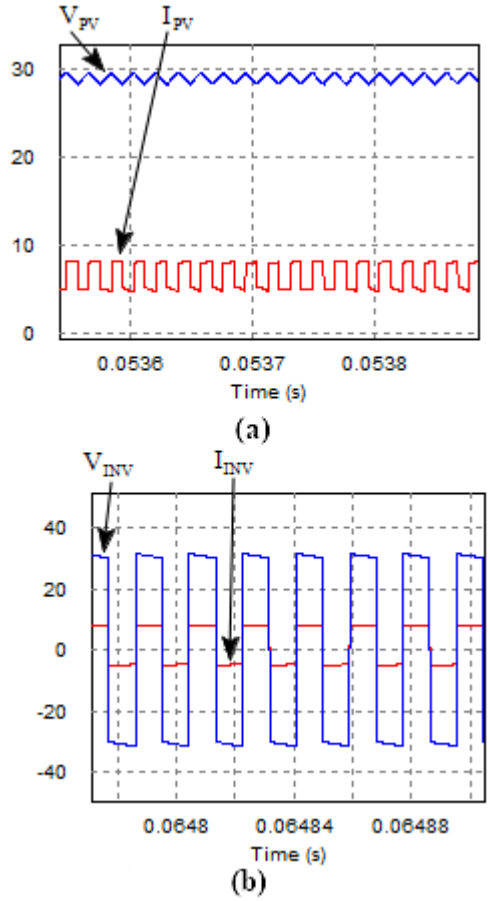

Figure 4. P-VG mode: waveforms of (a) PV module voltage and current, (b) HFI output voltage and current

The BDCC output voltage and current waveforms are presented in Fig. 6(c) which are observed as 232.7 V and 0.384 A respectively. It is observed from Fig. 6(b) and 6(c) that, the 55 kHz voltage is converted to 50 Hz using BDCC. BDCC output terminals are connected to a LC filter and are fed to the utility grid.

Utility grid voltage and current waveforms are presented in Fig. 6(d) which are observed as 229.96 V and 0.388 A respectively. The overall efficiency of the system while operating in forward PV-grid connected mode is observed as 96 %.

Simulation waveforms of the proposed system during PV-EV standalone mode (P-V mode) is presented in Fig. 7. During this mode, the PV panel generated power is sufficient to charge the EV battery only and the utility grid is isolated from the proposed system. Fig. 7(a) presents the PV panel voltage and current waveform while operating in this mode which is observed as 26.2 V and 3.7 A respectively.

The HF output voltage and current waveforms are presented in Fig. 7(b) which is observed as 26.2 V and 3.68 A respectively. The output of the inverter is fed to the rectifier. The rectifier output voltage and current is presented in Fig. 7(c) which is observed as 23.58 V and 4.07 A respectively.

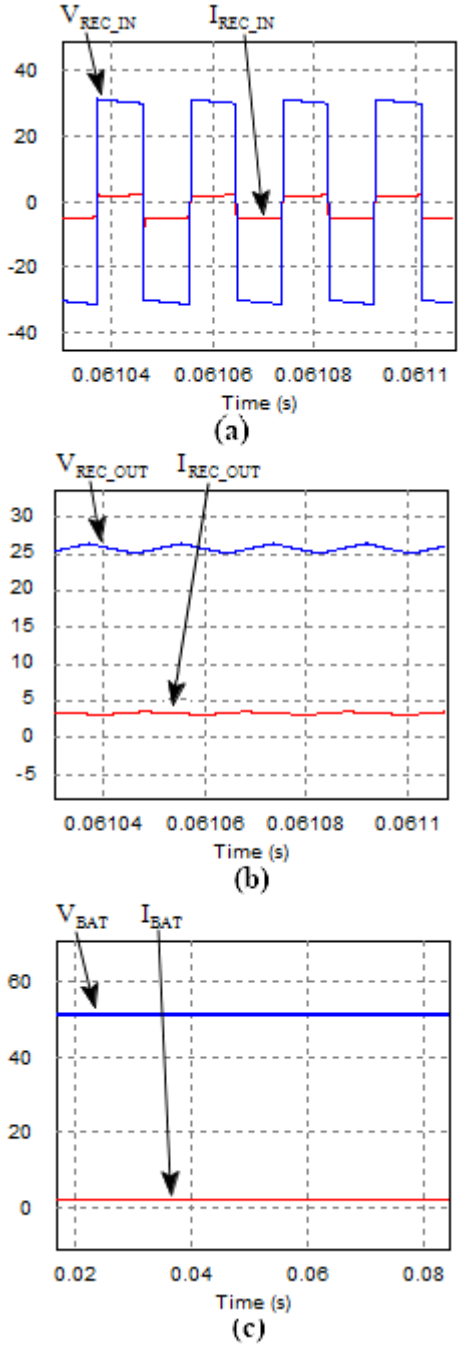

Figure 5. P-VG mode: waveforms of (a) Rectifier input voltage and current, (b) Rectifier output voltage and current, (c) EV battery voltage and current

In order to charge the EV battery, the rectifier output voltage of 23.58 V is boosted to 50 V by using the boost converter. Boost converter output voltage and current waveforms are presented in Fig. 7(d) which are observed as 50 V and 1.9 A respectively. The overall efficiency while operating in PV-EV standalone mode is found to be 98 %.

The proposed battery charging system operation during grid-EV reverse mode (G-V mode) of operation is simulated and the simulation study waveforms are presented in Fig. 8 and 9.

During this mode, PV module is isolated from the proposed system as the PV panel generated power is not sufficient to charge the EV battery. During G-V mode, the system operates using the utility grid power. Utility grid voltage and current waveforms are presented in Fig. 8(a) which is observed as 230 V and 0.434 A respectively. The utility grid voltage is converted to HFAC voltage using BDCC. The secondary side voltage and current waveforms of HFT are presented in Fig. 8(b) which are observed as 230 V and 0.421 A respectively. From Fig. 8(b) and 8(c), it is observed that, the HFT secondary voltage is stepped down from 230 V to 30 V at the primary side using HFT and fed to the rectifier. Rectifier input voltage of 30 V and current of 3.217 A are presented in Fig. 8(c).

Rectifier output voltage and current is observed as 28.05 V and 3.429 A respectively which are presented in Fig. 9(a). EV battery voltage and current waveforms during reverse mode are presented in Fig. 9(b) which are observed as 49.6 V and 1.92 A respectively. It is observed from Fig. 9 that, rectifier output voltage of 28.05 V is boosted to 49.6 V using boost converter in order to charge the EV battery. During G-V mode, the overall system efficiency is observed as 95 %.

Based on the simulation study of the system, a small scale laboratory prototype was fabricated and tested. Photograph of the experimental test bench of the fabricated prototype is shown in Fig. 10. PV module is emulated using Magna programmable dc supply for experimental investigation of the system. The high frequency inverter was fabricated employing 4 IRF540 MOSFET switches.

It converts constant dc voltage to 55 kHz square wave voltage. PIC18F45K20 Microcontroller is used to generate pulses for cycloconverter, inverter and the boost converter. The generated pulses are given to the BDCC, inverter and boost converter through 6N137 isolator and IR2130 gate driver circuit. The fabricated BDCC consists of 8, IRF840 MOSFET switches and diodes. A zero crossing detector (ZCD) circuit is fabricated employing TL082CN Opamp in order to synchronize the pulses of the BDCC with the utility grid voltage.

The experimental waveforms of the proposed system while operating in P-VG mode is given in Fig. 11-14. The experimental waveform of input voltage and current are presented in Fig. 11(a) which are observed as 28.9 V and 6.87 A respectively. HFI output voltage and current waveforms are presented in Fig. 11(b) which are observed as 28.7 V and 6.88 A respectively.

The rectifier input terminals and HFT primary terminals are connected in parallel with the output terminals of the HFI. The voltage and current waveforms at rectifier input terminals are presented in Fig. 11(c) which are observed as 28.7 V and 3.71 A respectively. The HFT primary side voltage and current waveforms are presented in Fig. 11(d) which are observed as 28.7 V and 3.12 A respectively. Experimental waveforms of rectifier output voltage and current are presented in Fig. 12(a) are observed as 26.9 V and 3.9 A respectively.

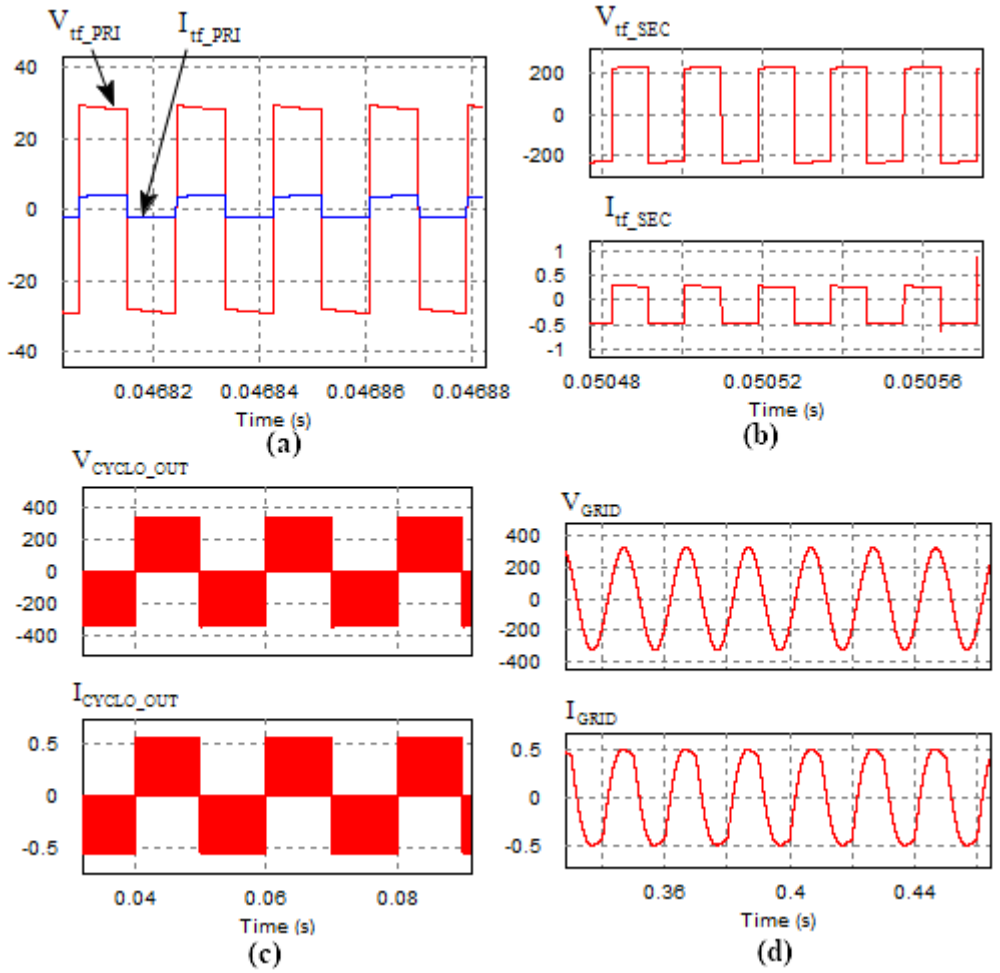

Figure 6. P-VG mode: waveforms of (a) HFT primary side voltage and current, (b) BDCC input voltage and current, (c) BDCCoutput voltage and current, (d) Utility grid voltage and current

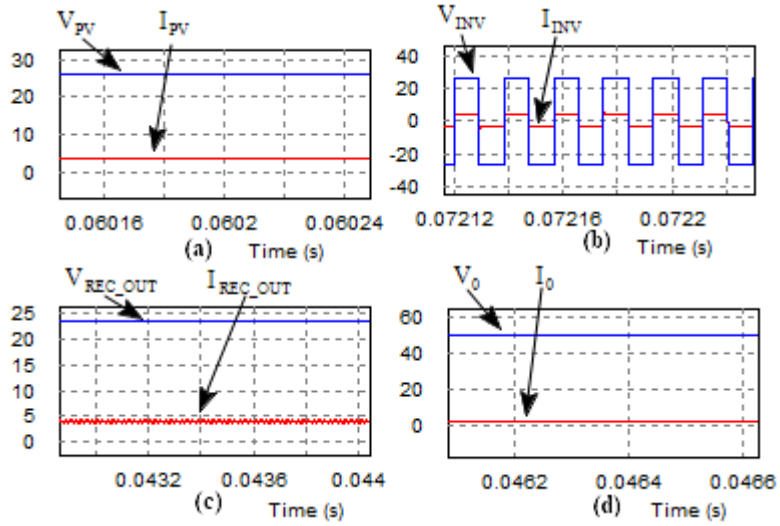

Figure 7. P-V mode: waveforms of (a) PV panel voltage and current, (b) HFI voltage and current, (c) rectifier output voltage and current, (d) EV battery voltage and current

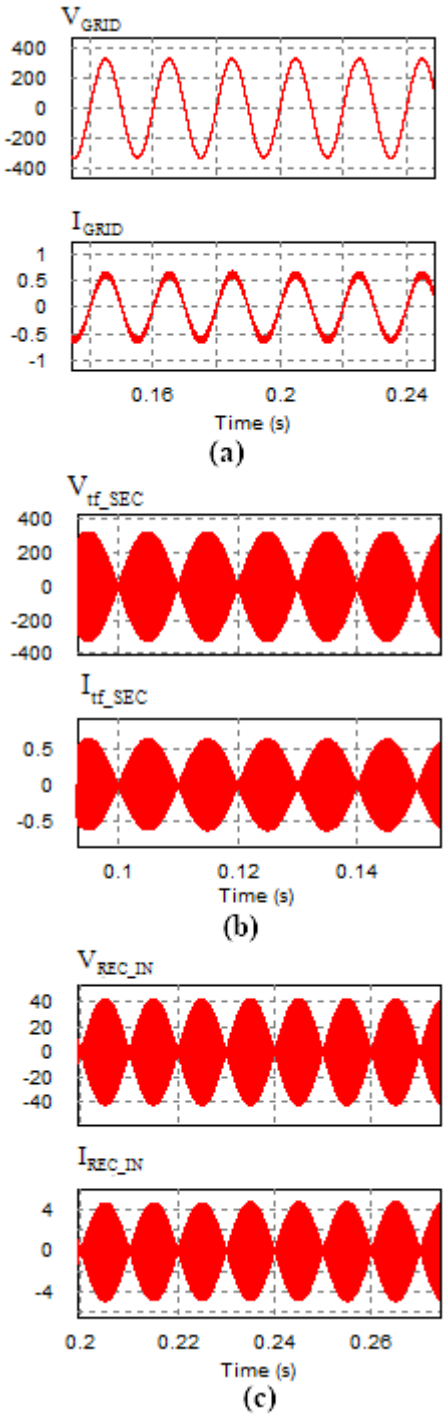

Figure 8. G-V mode: waveforms of (a) Utility grid voltage and current, (b) HFT secondary voltage and current, (c) Rectifier input voltage and current

The EV battery terminal voltage and current are presented in Fig. 12(b) which are observed as 50.4 V and 2.04 A respectively.

Step up transformer secondary side is connected to the BDCC input terminals. The BDCC input voltage and current waveforms during forward mode are presented in Fig. 13(a) which are observed as 232 V and 0.379 A respectively. Fig. 13(b) presents the BDCC output voltage and current waveforms of 232.2 V and 0.374 A respectively.

The utility grid voltage and current waveforms during forward mode are presented in Fig. 13(c) which are observed as 231.2 V and 0.375 A respectively. The harmonic spectrum of BDCC output voltage and current before filter are presented in Fig. 14(a) & 14(b) which is observed as 42.5 % and 42.4 % respectively. The total harmonic distortion (THD) value is very high as compared to IEEE standard. Therefore, an LC filter is employed to reduce the voltage and current THD. The grid voltage and current harmonics spectrum after the filter are presented in Fig. 14(c) & 14(d) respectively which are having a lesser THD value as per the IEEE standard. The overall system efficiency in P-VG mode operation is found to be 95.6 %.

Proposed system operation in P-V mode is presented in Fig. 15. In this mode the utility grid is isolated from the system as the PV panel generated power is sufficient only to charge the EV battery. Fig. 15(a) presents the voltage and current waveforms of PV panel which are observed as 25.8 V and 3.68 A respectively. HFI output voltage and current waveforms are presented in Fig. 15(b) which are observed as 25.8 V and 3.65 A respectively. The rectifier output voltage and current waveforms are presented in Fig. 15(c) which are observed as 23.9 V and 3.88 A respectively. The rectifier output voltage of 23.9 V is boosted to 51 V in order to charge the EV battery. The EV battery terminals voltage and current waveforms are presented in Fig. 15(d) which are observed as 51 V and 1.8 A respectively. The system overall efficiency during this mode is observed as 97 %.

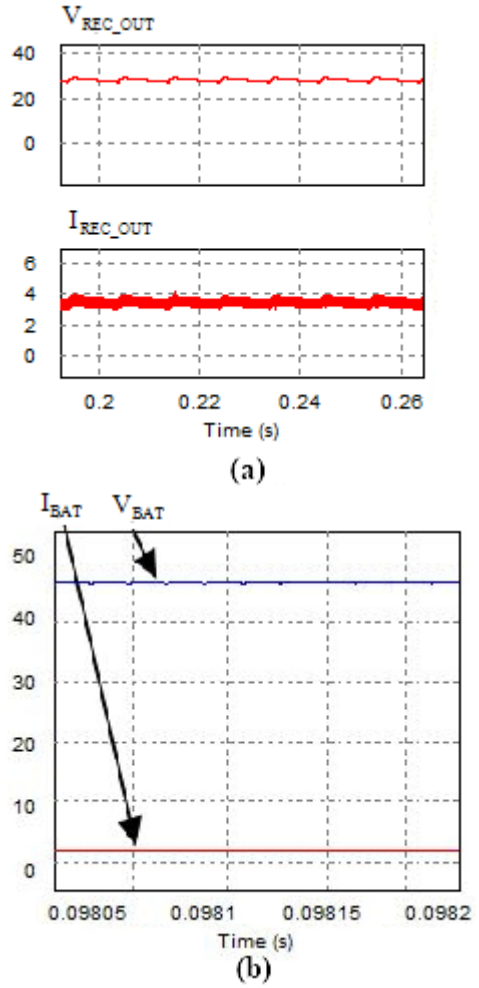

Figure 9. G-V mode: waveforms of (a) Rectifier output voltage and current, (b) EV battery voltage and current

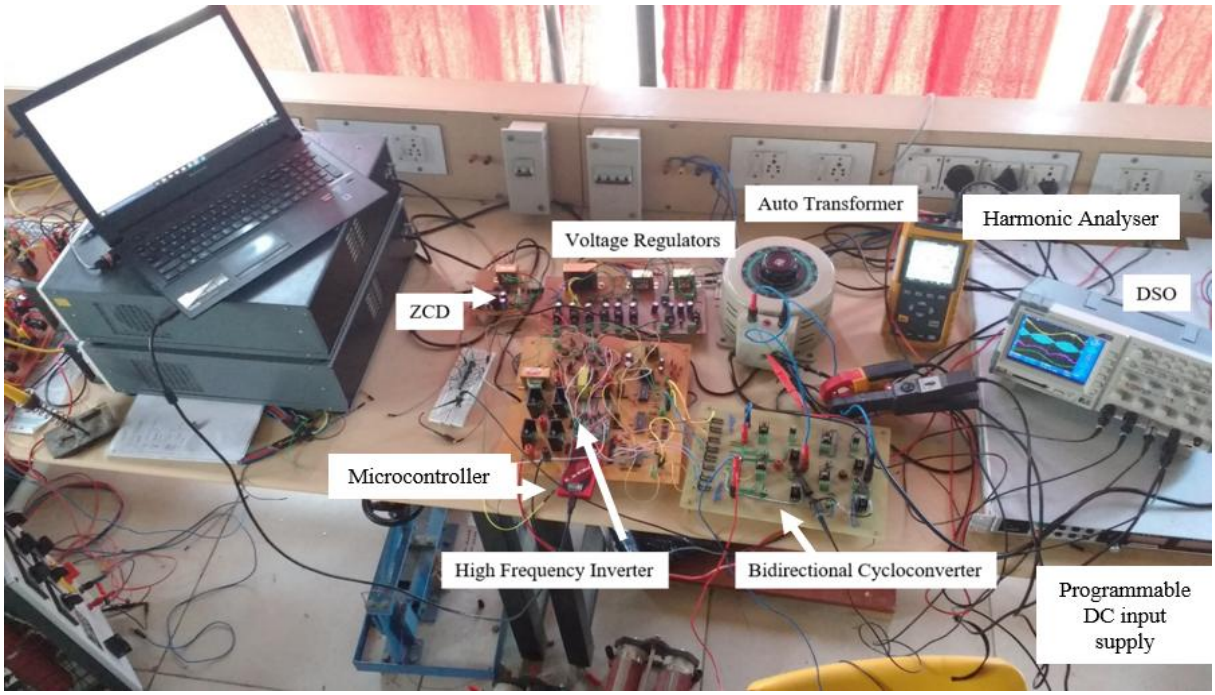

Figure 10. Photograph of the experimental test bench of the proposed EV battery charger

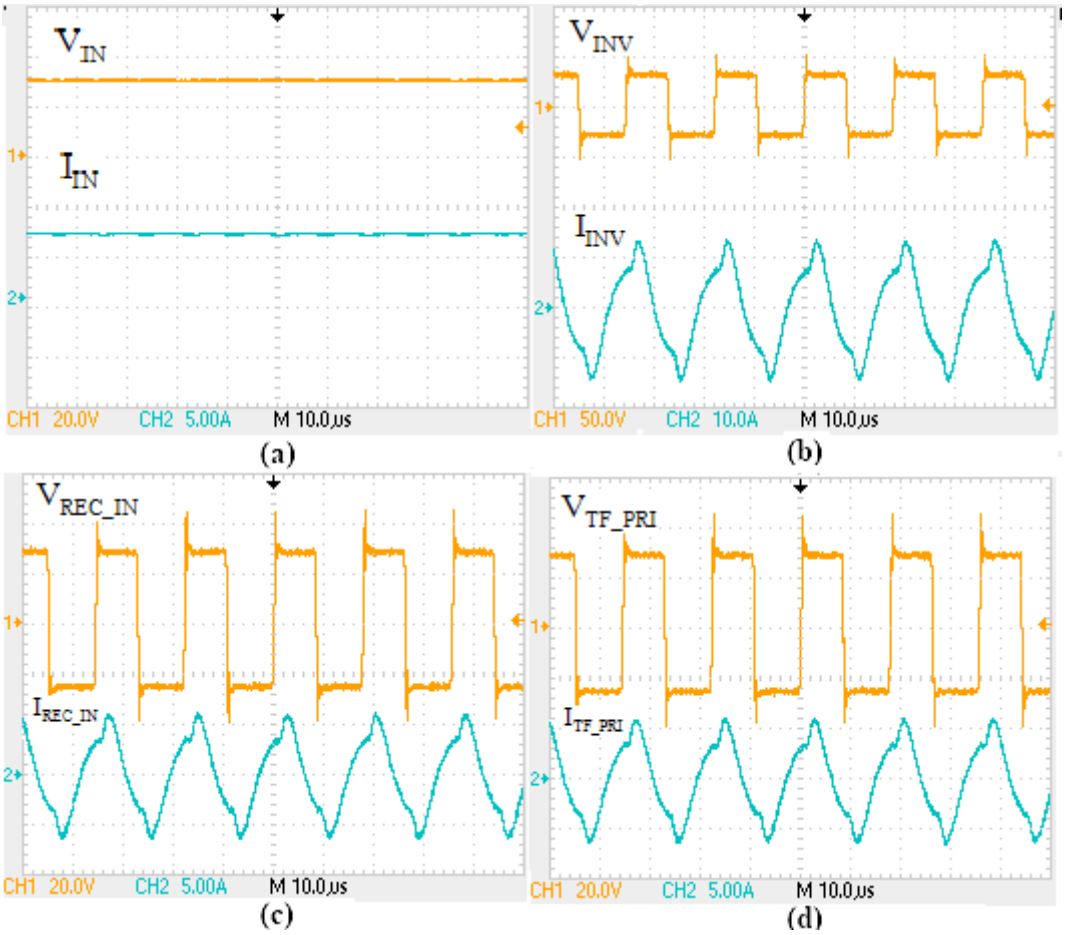

Figure 11. P-VG mode: Waveforms of (a) Input voltage and current, (b) HFI voltage and current, (c) Rectifier input voltage and current, (d) HFT primary voltage and current

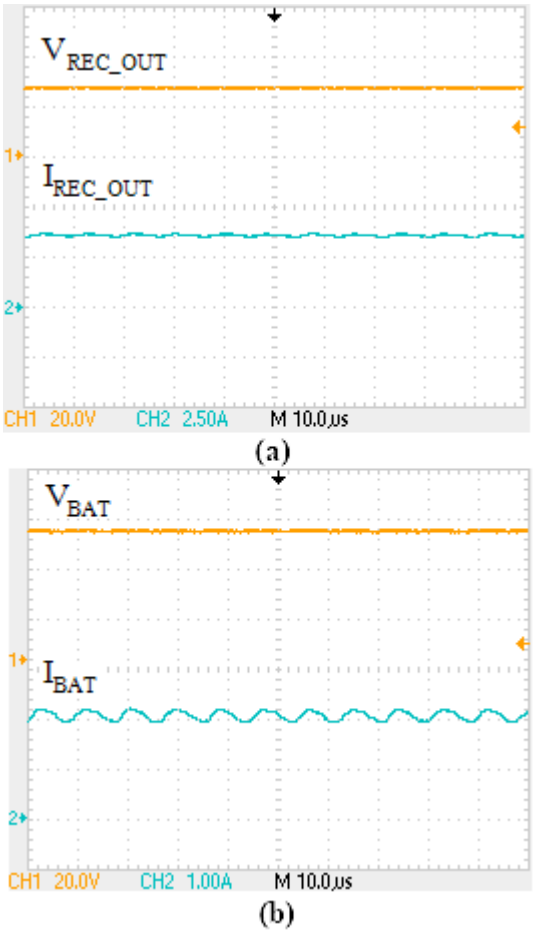

Figure 12. P-VG mode: waveform of (a) Rectifier output voltage and current, (b) EV battery voltage and current

In grid-EV reverse mode, the utility grid acts as a source and the input dc source is isolated from the proposed system. The experimental results of the grid voltage and current during grid-EV reverse mode are presented in Fig. 16(a). Grid voltage and current value are observed as 230.4 V and 0.434 A respectively. The experimental waveforms of the HFT secondary side terminals are presented in Fig. 16(b) which are observed as 233 V and 0.412 A respectively. The HFT primary side is connected in parallel with the rectifier input terminals. Experimental waveforms of the HFT primary side voltage and current are presented in Fig. 16(c) and are observed as 31.2 V and 3.04 A respectively. The experimental waveforms of the rectifier output voltage and current are presented in Fig. 17(a) which are observed as 26.9 V and 3.52 A respectively during reverse mode. The boost converter output terminals voltage and current waveforms are presented in Fig 17(b) which are observed as 50 V and 1.89 A respectively. The overall system efficiency in Gid-EV reverse mode is found to be 94.5 %.

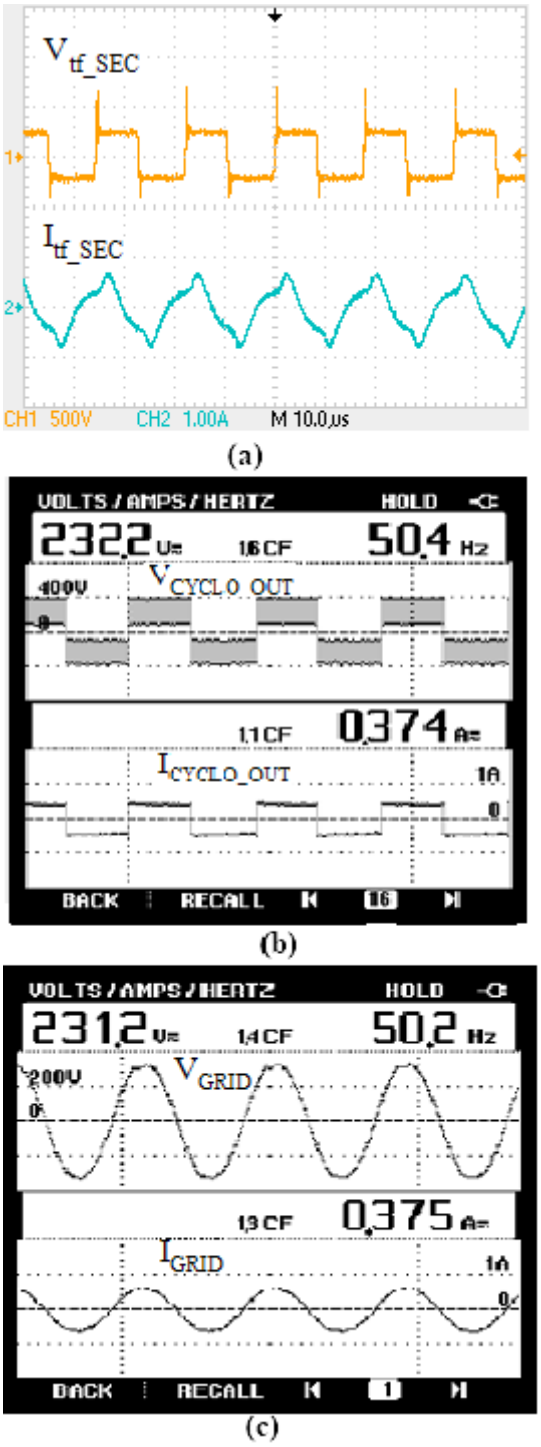

Figure 13. P-VG mode: waveform of (a) HFT secondary side voltage and current, (b) BDCC output voltage and current, (c) Grid voltage and current

Similarity between the simulation results and experimental investigation results proves the effectiveness of the proposed system.

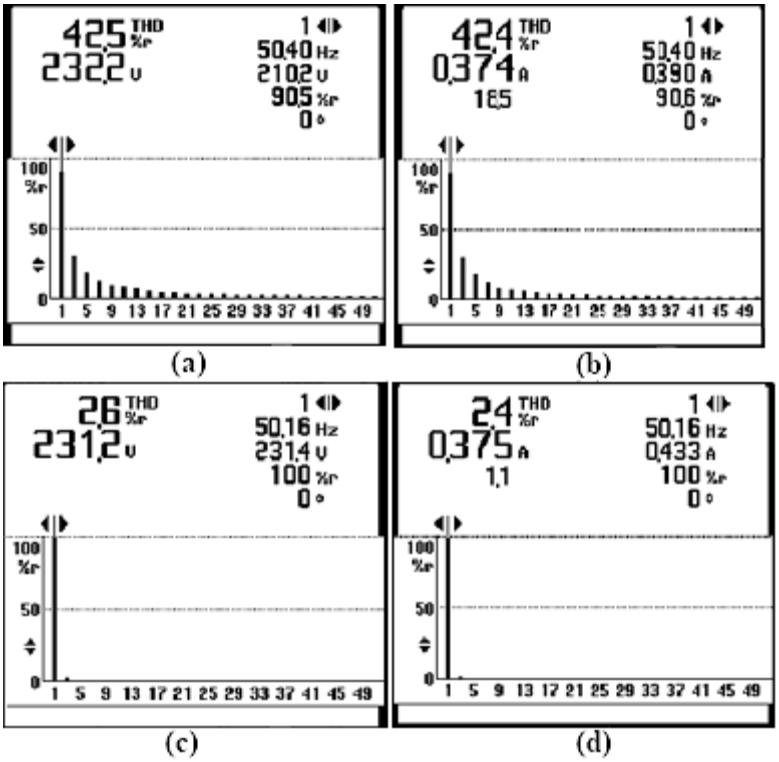

Figure 14. P-VG mode: Harmonic spectrum of (a) BDCC output voltage, (b) BDCC output current, (c) Grid voltage, (d) Grid current

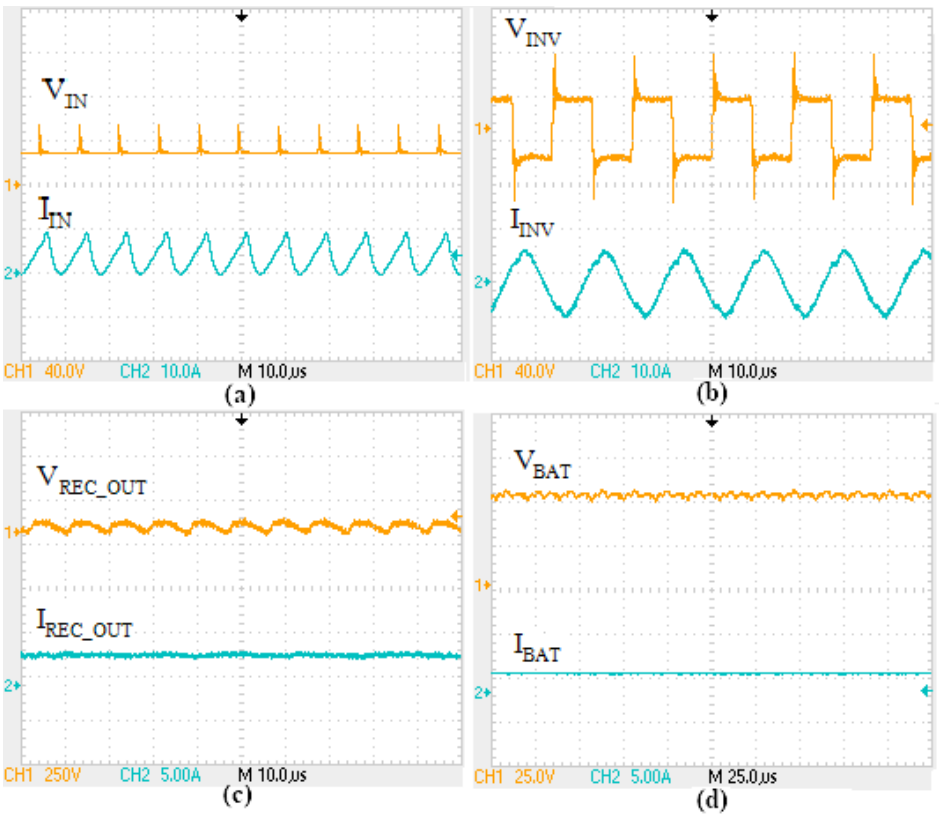

Figure 15. P-V mode: waveforms of (a) Input voltage and current, (b) HFI output voltage and current, (c) Rectifier output voltage and current and (d) EV battery terminals voltage and current

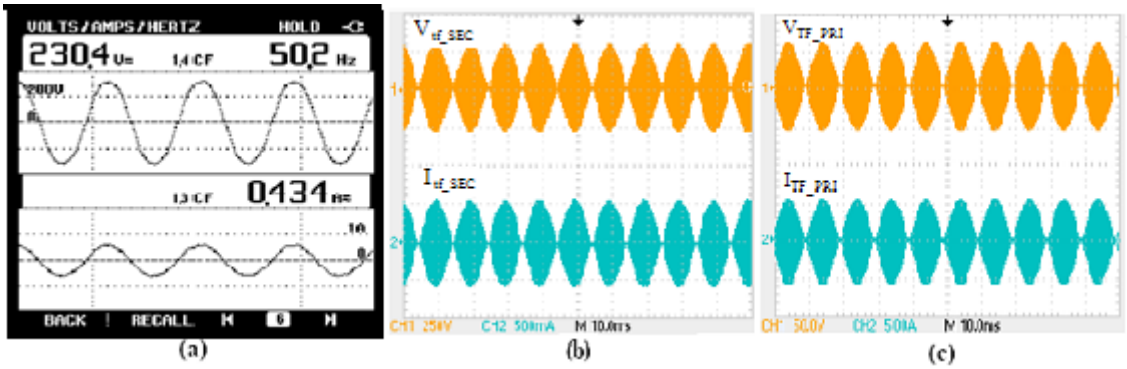

Figure 16. G-V mode: waveform of (a) Utility grid voltage and current, (b) HFT secondary side voltage and current, (c) HFT primary side voltage and current

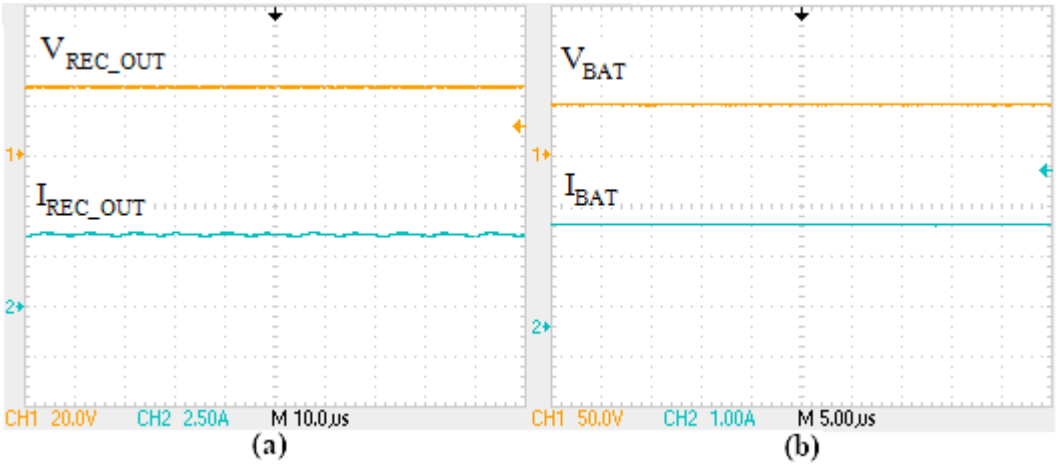

Figure 17. G-V mode: waveform of (a) Rectifier output voltage and current, (b) EV battery terminals voltage and currents

IV. CONCLUSION

The proposed system enables uninterrupted charging of an EV battery from PV module or utility grid. PV module is employed as primary source of energy and utility grid power is used as the secondary source in this battery charging system. In order to reduce the size of the passive elements employed in this proposed system, HF power conversion is used. The BDCC is employed in this battery charging system to enable bidirectional power flow from PV module to grid and from grid to vehicle. The designed system is simulated using PSIM software and the hardware investigation is performed. Homogeneity of experimental investigation results with the simulated results validates the efficacy of the proposed EV battery charging system.

REFERENCES

1. T. H. Ortmeyer and P. Pillay, "Trends in transportation sector technology energy use and greenhouse gas emissions," *Proc. IEEE*, 89(12), 2001, pp. 1837–1847.
2. Krithiga, S & Sujitha, N. (2015). A hybrid PV system using single phase bridgeless interleaved converter for electric vehicle energy storage applications. *International Journal of Applied Engineering Research*, 10(12), 2015, pp. 37168-37174.
3. Krithiga S. and Partha Sarathi Subudhi, "PV fed Water Pumping System in a Smart Home," *Int. J. Eng. Technol.*, 7(3), 2018, pp. 1565-69.
4. A. R. Bhatti, Z. Salam, M. J. B. A. Aziz, and K. P. Yee, "A critical review of electric vehicle charging using solar photovoltaic," *Int. J. Energy Res.*, 40(4), 2016, pp. 439–461.
5. Y.-M. Wi, J.-U. Lee, and S.-K. Joo, "Electric vehicle charging method for smart homes/buildings with a photovoltaic system," *IEEE Trans. Consum. Electron.*, 59(2), 2013, pp. 323–328.
6. K. A. Kalwar, M. Aamir, and S. Mekhilef, "Inductively coupled power transfer (ICPT) for electric vehicle charging - A review," *Renew. Sustain. Energy Rev.*, 47, 2015, pp. 462–475.
7. S. Krithiga and N. Ammasai Gounden, "Investigations of an improved PV system topology using multilevel boost converter and line commutated inverter with solutions to grid issues," *Simul. Model. Pract. Theory*, vol. 42, pp. 147–159, 2014.
8. G. R. Chandra Mouli, P. Bauer, and M. Zeman, "System design for a solar powered electric vehicle charging station for workplaces," *Appl. Energy*, 168, 2016, pp. 434–443.
9. C. Youssef, E. Fatima, E. Najia, and A. Chakib, "A technological review on electric vehicle DC charging stations using photovoltaic sources," *IOP Conf. Ser. Mater. Sci. Eng.*, 353(1), 2018, pp. 1–9.
10. M. Yilmaz and P. T. Krein, "Review of Battery Charger Topologies, Charging Power Levels, and Infrastructure for Plug-In Electric and Hybrid Vehicles," *IEEE Trans. Power Electron.*, 28(5), 2013, pp. 2151–2169.
11. Y. Ota, H. Taniguchi, H. Suzuki, T. Nakajima, J. Baba, and A. Yokoyama, "Implementation of grid-friendly charging scheme to electric vehicle off-board charger for V2G," in *2012 3rd IEEE PES Innovative Smart Grid Technologies Europe (ISGT Europe)*, 2012, pp. 1–6.
12. A. Agarwal and V. Agarwal, "FPGA based variable frequency AC to AC power conversion," *Electr. Power Syst. Res.*, 90, 2012, pp. 67–78.
13. A. Agarwal and V. Agarwal, "Design of Delta-Modulated Generalized Frequency Converter," *IEEE Trans. Ind. Electron.*, 57(11), 2010, 3724–3729.
14. S. Krithiga, D. R. B. B. Jose, H. R. Upadhya, and N. A. Gounden, "Grid-Tied Photovoltaic Array Using Power Electronic Converters with Fuzzy Logic Controller for Maximum Power Point Tracking," *Aust. J. Electr. Electron. Eng.*, vol. 9, no. 4, pp. 393–400, Jan. 2012.
15. S. Krithiga and N. Ammasai Gounden, "An Improved Power Electronic Controller with Unity Power Factor for a Single-Stage Grid-Tied PV System," *Arab. J. Sci. Eng.*, vol. 39, no. 10, pp. 7173–7182, Oct. 2014.
16.

AUTHORS PROFILE

Partha Sarathi Subudhi was born in Bhubaneswar, India in 1991. He received his B.Tech. degree in Electrical Engineering from Konark Institute of Science and Technology, Biju Patnaik University of Technology, Bhubaneswar, India in 2012 and M.Tech. degree in Power Electronics and Drives from Vellore Institute of Technology (VIT), Chennai, Tamil Nadu, India in 2015. He is currently pursuing his Ph. D. degree in Electrical and Electronics Engineering in Vellore Institute of Technology (VIT), Chennai, Tamil Nadu, India. His field of interest includes Renewable energy systems, Power electronic converters, Plug-in and Wireless Power Transfer and Electric Vehicle battery charging applications, Hybrid Converter.

Krithiga S. received the B.E. degree in Electrical and Electronics Engineering from P.S.G. College of Technology, Bharathiyar University, Coimbatore, Tamil Nadu, India, in 2003 and M.Tech. degree from National Institute of Technology, Tiruchirappalli, Tamil Nadu, India, in 2008. She received Ph. D. degree in the Department of Electrical and Electronics Engineering from National Institute of Technology (NIT), Tiruchirappalli, Tamil Nadu, India, in 2014. From 2004 to 2006, she was a Research Assistant with National Institute of Technology (NIT), Tamil Nadu, India and from 2009 to 2010, She was an Assistant professor with Electrical and Electronics Engineering Department in B.S. Abdur Rahman Crescent University (formerly B.S.A. Crescent Engineering College), Chennai, Tamil Nadu, India. Since 2014, she is an Associate Professor with School of Electrical Engineering, Vellore Institute of Technology, Chennai, Tamil Nadu, India. Her research interests are Renewable energy systems and its applications, power electronic converters and Electric Vehicle battery charging systems.